

Accepted Article

Antimicrobial activity and mechanism of action of a thionin-like peptide from *Capsicum annuum* fruits and combinatorial treatment with fluconazole against *Fusarium solani*

Gabriel B. Taveira^a, Érica O. Mello^a, André O. Carvalho^a, Mariana Regente^b, Marcela Pinedo^b, Laura de La Canal^b, Rosana Rodrigues^c, Valdirene M. Gomes^{a*}

^aLaboratório de Fisiologia e Bioquímica de Microrganismos, Centro de Biociências e Biotecnologia, Universidade Estadual do Norte Fluminense, Campos dos Goytacazes 28013-602, RJ, Brazil.

^bInstituto de Investigaciones Biológicas, Universidad Nacional de Mar del Plata- CONICET, Funes 3250, 7600 Mar del Plata, Argentina.

^cLaboratório de Melhoramento Genético Vegetal, Centro de Ciências e Tecnologias Agropecuárias, Universidade Estadual do Norte Fluminense, Campos dos Goytacazes 28013-602, RJ, Brazil.

Running head: Antifungal thionin from *Capsicum annuum* fruits

* Corresponding author. Fax: +55-22-27396659

E-mail address: valmg@uenf.br (Gomes, V.M.)

This article has been accepted for publication and undergone full peer review but has not been through the copyediting, typesetting, pagination and proofreading process which may lead to differences between this version and the Version of Record. Please cite this article as an 'Accepted Article', doi: 10.1002/bip.23008

Abstract

Many *Fusarium* species are able to cause severe infections in plants as well as in animals and humans. Therefore, the discovery of new antifungal agents is of paramount importance. *CaThi* belongs to the thionins, which are cationic peptides with low molecular weights (~ 5 kDa) that have toxic effects against various microorganisms. Herein, we study the mechanism of action of *CaThi* and its combinatory effect with fluconazole (FLC) against *Fusarium solani*. The mechanism of action of *CaThi* was studied by growth inhibition, viability, plasma membrane permeabilization, ROS induction, caspase activation, localization and DNA binding capability, as assessed with Sytox green, DAB, FITC-VAD-FMK, *CaThi*-FITC and gel shift assays. The combinatory effect of *CaThi* and FLC was assessed using a growth inhibition assay. Our results demonstrated that *CaThi* present a dose dependent activity and at the higher used concentration (50 $\mu\text{g mL}^{-1}$) inhibits 83% of *F. solani* growth, prevents the formation of hyphae, permeabilizes membranes, induces endogenous H_2O_2 , activates caspases, and localizes intracellularly. *CaThi* combined with FLC, at concentrations that alone do not inhibit *F. solani*, result in 100% death of *F. solani* when combined. The data presented in this study demonstrate that *CaThi* causes death of *F. solani* via apoptosis; an intracellular target may also be involved. Combined treatment using *CaThi* and FLC is a strong candidate for studies aimed at improved targeting of *F. solani*. This strategy is of particular interest because it minimizes selection of resistant microorganisms.

Keywords: Antimicrobial peptides, Synergism, Fungi, Membrane permeability

INTRODUCTION

Significant production losses to global crops caused by plant pathogens such as viruses, bacteria, fungi and other organisms is a great concern for food security. These losses represent more than 10% of global food production yields.^{1,2} In Brazilian agriculture alone, pesticide use totals US \$ 1.6 billion/year, corresponding to an alarming volume of pollutants released every day. Such pollution is implicated in numerous adverse effects, including toxicity to humans and non-target organisms.^{3,4} Paradoxically, despite the increasing use of pesticides, there is an increase in plant diseases caused by fungi that are becoming more resistant to currently available fungicides. Therefore, the discovery of new antifungal agents, particularly those endogenous to plants, is of paramount importance.⁵⁻⁷

Over the last decade, many studies have focused on antimicrobial proteins and peptides from various plant sources. Antimicrobial peptides (AMPs) are produced by several species: including bacteria, insects, plants, vertebrates, and have been characterized from almost all organisms, ranging from prokaryotes to humans.⁸⁻¹⁰ AMPs participate in the innate immune response, which is the first line of defence for most organisms against infection.¹¹

Among these AMPs are thionins, which belong to a family of plant AMPs. Thionins are cationic peptides (pI > 8) with low molecular weights (~ 5 kDa) and which are rich in arginine, lysine and cysteine residues. Thionins have sequence and structural similarities as well as toxic effects against microorganism, plant and animal cells.^{11,12} In 1942, Balls *et al.*¹³ crystallized and purified a toxic molecule from wheat endosperm (*Triticum aestivum*). This protein material with a low molecular weight and a high sulphur content, designated as purothionine, is the first recorded thionin. Recently, thionins have been isolated from a wide variety of monocotyledon and dicotyledon

plant species.¹⁴ Many thionins are toxic to gram-positive and gram-negative bacteria, yeast, phytopathogenic fungi, protozoa and insects.^{11,14-17} The mechanism of action of thionins on microorganisms was first investigated in *Saccharomyces cerevisiae*. A thionin from *T. aestivum* seeds caused permeabilization of yeast cells, as shown by leakage of ions, such as K^+ and PO_4^{3-} , and some cellular components into the culture medium.¹⁸ Indirect experimental evidence indicates that thionins form pores and/or disintegrate of the plasma membrane, followed by massive depolarization and loss of cytoplasmic components by increasing the thionin concentration in the medium. However, the precise mechanism of thionin toxicity remains unknown.^{14, 19} Thionins have strong toxic effects on microorganisms, as such they are excellent candidates for the development of new substances for crop protection and antifungal treatments of human infection.^{12, 20}

In previous reports,^{21, 22} our group isolated a thionin-like peptide, named *CaThi*, from *Capsicum annuum* fruits. This peptide had strong antimicrobial activity against *Escherichia coli* and *Staphylococcus aureus* as well as candidacidal activity against six *Candida* species. Some aspects of the mechanism of action of *CaThi* against important human pathogens were also described; for example, *CaThi* has a synergistic effect against yeasts when combined with FLC. FLC is a triazole mostly used for medical treatment of fungal infections, especially by *Candida*.²³ However, several triazoles are used in plant protection²⁴ and for several decades, agricultural researchers have known that extensive use of triazoles results in contamination of air, plants and soil.²⁵

In this work, we evaluate the mechanism of action and synergistic activity of *CaThi* combined with FLC on the growth of the important pathogenic plant fungus *F. solani*. This saprophytic fungus causes disease in plants, animals and humans, and in the

last decade has caused an increasing number of infections in immunocompromised patients.²⁶⁻²⁸ This study contributes to a better understanding of AMP-pathogen interactions and how AMPs are used by plants to control fungal invasion, helping to establish guidelines for the implementation of AMPs in the treatment of fungal disease.

MATERIAL AND METHODS

Biological materials

Capsicum annuum L. (accession UENF1381) fruits were provided by the *Laboratório de Melhoramento Genético Vegetal* at the *Centro de Ciências e Tecnologias Agropecuárias, Universidade Estadual do Norte Fluminense - Darcy Ribeiro (UENF)*, Campos dos Goytacazes, Rio de Janeiro, Brazil. Pepper plants were grown in a growth chamber at 28 °C and 80% relative humidity with a 16 h light/8 h dark photoperiod. Seeds were sown in trays of 72 cells with commercial substrate fertilized with NPK, which provides 4% nitrogen, 14% phosphorus and 8% potassium, and irrigated once a day. After 20 days post-emergence, plants were transplanted to the greenhouse and grown under the same treatment.

The fungus *Fusarium solani* f. sp. *eumartii*, isolate 3122 (EEA-INTA, Balcarce, Argentina) was provided by the *Instituto de Investigaciones Biológicas, Universidad Nacional de Mar del Plata*, Mar del Plata, Argentina. The fungus was maintained on Sabouraud agar (1% peptone, 2% glucose, and 1.7% agar-agar) (Merck) supplemented with 100 µg mL⁻¹ ampicillin.

Extraction and purification of CaThi

CaThi extraction and purification were accomplished as described by Taveira *et al.*²¹ Briefly, eighty grams of *C. annuum* fruits (without seeds) were extracted for 2 h (at 4

°C) with 400 mL of extraction buffer (10 mM Na₂HPO₄, 15 mM NaH₂PO₄, 100 mM KCl, 1.5% EDTA, pH 5.4) (Sigma). Extracted proteins were precipitated with 0 and 70% relative ammonium sulphate (472 g L⁻¹) (Merck) saturation and centrifuged at 20,000 x g for 30 min at 4 °C. Precipitates were re-dissolved in 5 mL of distilled water and heated at 80 °C for 15 min. The resulting suspension was clarified by centrifugation, as before, and the supernatant was extensively dialyzed against distilled water. The extract was submitted to fractionation using chromatographic methods. The retention time to recover *CaThi* using reversed-phase chromatography with a μ RPC C2/C18 column (ST 4·6/100) (GE Healthcare) was 37.87 min.¹⁶ The column was equilibrated and run with solvent A (aqueous 0.1% TFA) (Sigma) for the first 8 min followed by a gradient of solvent B (100% propanol (Sigma) in 0.1% TFA) for 75 min. The flow rate was 0.5 mL min.

Effect of *CaThi* on fungal growth

The fungus *F. solani* was transferred from stock and placed in a Petri dish containing Sabouraud agar and grown for approximately 15 days at 25 °C. After this period, 10 mL of Sabouraud broth were poured over the plate containing the fungus, and the conidia were released with the aid of a Drigalski spatula. This suspension was filtered through gauze to prevent the passage of mycelial debris that may have been in solution with the conidia. These conidia were quantified in a Neubauer chamber (Laboroptik) under an optical microscope. A quantitative assay for fungal growth inhibition was performed following the protocol developed by Broekaert *et al.*²¹ with modifications as follows. To verify the effect of *CaThi* on *F. solani* growth, 1x10⁴ conidia mL⁻¹ in 200 μ L of Sabouraud broth were incubated at 25 °C in 96-well microplates (Nunc) in the presence of *CaThi* at a concentration of 50, 25 and 12.5 μ g mL⁻¹. Optical readings at 620 nm

were collected at the start and every 6 h for 60 h. Fungal growth without the addition of *CaThi* was also determined. Graphs of absorbance versus time were plotted. The experiments were repeated three times in triplicate, and the inhibition percentage was calculated by the formula according to Vieira *et al.*³⁰ with the following modifications: the inhibition percentages were assessed against a control representing 100% growth based on the formula $[100 - (CaThiABS620 \times 100/ cABS620)]$, where *CaThiABS620* was the average absorbance reading at 620 nm of *CaThi*-treated cells at 60 h and *cABS620* was the average absorbance reading at 620 nm of the control cells at 60 h. These fungal growth inhibition data were evaluated by One-way ANOVA, and differences of the mean at $p < 0.05$ were considered significant. All statistical analyses were performed using GraphPad Prism software (version 5.0 for Windows). The IC_{50} was calculated based on a linear regression curve and it is defined as the *CaThi* concentration required to inhibits 50% of microorganism growth in the condition tested.

Viability assay

To assess the effect of *CaThi* on *F. solani* conidia viability, 1×10^4 conidia mL^{-1} in sterile water, were incubated in the presence of $50 \mu g mL^{-1}$ of *CaThi* at 25 °C for 24 h in 96-well microplates (Nunc). Control cells without *CaThi* were washed once and diluted 100-fold in sterile water, and a 100- μL aliquot from this dilution was spread over the surface of Sabouraud agar medium (Petri dish 90 x 15 mm) with a Drigalski spatula and grown at 25 °C for 48 h. At the end of this period, colony forming units (CFU) were determined and the Petri dishes were photographed. The same procedure was used for *F. solani* conidia treated with *CaThi*. The experiments were performed in duplicate, and the results shown were calculated assuming that the control represents 100% of conidia viability, using the formula $([100 - (a \times 100/b)])$ where *a* was the

average CFU of treated sample and b was the average CFU of control sample according to Vieira *et al.*³⁰

Plasma membrane permeabilization

Fungal plasma membrane permeabilization was measured by Sytox green uptake as described previously by Thevissen *et al.*³¹. Sytox green is a dye that only passes through cells when the plasma membrane is structurally compromised. Once inside the fungal cytoplasm, it binds to nucleic acids to give a fluorescent signal. Accordingly, this dye can be used to verify fungal plasma membrane permeabilization. This assay was performed as described in the section “**Effect of CaThi on fungal growth**” with the indicated differences: the fungus *F. solani* (1×10^4 conidia mL^{-1}) was incubated in the presence of CaThi at a concentration of $50 \mu\text{g mL}^{-1}$ for 12, 24, 48 and 60 h. After these periods, 100- μL aliquots of the fungal cell suspension were incubated with $0.2 \mu\text{M}$ Sytox green and $10 \mu\text{g mL}^{-1}$ of propidium iodide in 1.5-mL microcentrifuge tubes for 15 min at $25 \text{ }^\circ\text{C}$ with constant agitation. The cells were observed under an optical microscope (Axioplan.A2, Zeiss) equipped with a fluorescence filter set for fluorescein detection (excitation wavelengths, 450 to 490 nm; emission wavelength, 500 nm). All images were acquired with the same exposure time.

Determining the induction of hydrogen peroxide in *F. solani* conidia

To investigate whether CaThi is able to cause the production of endogenous hydrogen peroxide in *F. solani* conidia, we used 3, 3'-diaminobenzidine (DAB) (Sigma). The DAB is oxidized immediately and locally by hydrogen peroxide and peroxidase, and the presence of peroxides is observed as a dark-brown colour due to the formation of an insoluble precipitate at the reaction site. Initially, a DAB solution 1 mg mL^{-1} was

prepared in water with constant agitation overnight and protected from light, as described previously by Thordal-Christensen *et al.*³² and Liu *et al.*³³ The fungal conidia (1×10^4 cell mL^{-1}) were incubated with *CaThi* ($50 \mu\text{g mL}^{-1}$) in 1.5-mL microcentrifuge tubes in a final volume of 100 μL of Sabouraud broth and DAB at a final concentration of 0.5 mg mL^{-1} . Samples were measured every 10 min for a total time of 60 min. For negative controls, conidia were incubated in the absence of *CaThi*, and as positive controls, conidia were incubated with 200 mM of hydrogen peroxide. Observations were conducted using optical microscopy.

Detection of caspase activity induced by *CaThi* in *F. solani*

Detection of caspase activity was performed using the *in situ* marker CaspACE FITC-VAD-FMK (Promega) as described by the manufacturer. The marker FITC-VAD-FMK is an analogue of the caspase inhibitor Z-VAD-FMK (carbobenzoxy-valyl-alanyl-aspartyl-[O-methyl]-fluoromethylketone). The N-terminal carbobenzoxy (Z) is replaced by fluorescein isothiocyanate (FITC), creating a green fluorescent label for apoptosis. This assay was performed as described in the section “**Effect of *CaThi* on fungal growth**” with the indicated differences: After incubation for 12 and 24 h with *CaThi*, *F. solani* conidia were suspended, washed once in 500 μL of PBS (10 mM NaH_2PO_4 , 0.15 M NaCl) pH 7.4 and suspended in 50 μL of staining solution containing 50 μM of FITC-VAD-FMK and $10 \mu\text{g mL}^{-1}$ of propidium iodide. After 20 min incubation at 25 $^\circ\text{C}$ under constant agitation at 500 rpm, the cells were again washed in 500 μL PBS and resuspended in 20 μL of PBS. The negative control cells (in the absence of *CaThi*) underwent the same treatment as cells treated with the peptide. The cells were observed under an optical microscope (Axioplan.A2, Zeiss) equipped with a fluorescence filter

set for fluorescein detection (excitation wavelengths, 450-490 nm; emission wavelength, 500 nm). All images were acquired with the same exposure time.

Localization of CaThi in *F. solani* conidia

To verify whether CaThi is able to enter *F. solani* cells, we coupled CaThi to fluorescein isothiocyanate (FITC) and monitored the interaction of FITC-tagged CaThi with *F. solani* by optical microscopy. Initially, 100 μg of CaThi was coupled to FITC as described previously by Taveira *et al.*²² After coupling, 20 $\mu\text{g mL}^{-1}$ of CaThi-FITC was incubated with *F. solani* cells in 96-well microplates. After 60 h of incubation, an aliquot of fungal suspension was removed and incubated with 50 $\mu\text{g mL}^{-1}$ of 4',6-diamidino-2-phenylindole dihydrochloride (DAPI) for 10 min to stain nuclei. Cells were analysed using a DIC optical microscope (Axioplan.A2, Zeiss) equipped with a fluorescent filter set for detection of fluorescein (excitation wavelengths, 450-490 nm; emission wavelength, 500 nm) and DAPI (excitation wavelengths, 385-400 nm; emission wavelength, 450-465 nm).

Analysis of DNA binding capability of CaThi

F. solani DNA was extracted using the "DNeasy Plant Mini Kit" (Qiagen) from a culture of *F. solani* grown on Sabouraud broth for 48 h, and the extracted DNA was quantified using a NanoDrop 2000 (Applied Biosystems). The mobility shift test is based on the binding of DNA to proteins that results in a complex with a different electrophoretic mobility than free DNA. The mobility of the complex is observed in the agarose gel as slower migration relative to free DNA.

The assay was performed as described by Park *et al.*³⁴ Briefly, a 0.8% agarose gel was prepared according to Sambrook and Russel.³⁵ One hundred nanograms of fungal DNA

were incubated with 50, 25 and 12.5 $\mu\text{g mL}^{-1}$ of *CaThi* plus 20 μL binding buffer (5% glycerol, 10 mM Tris-HCl pH 8.0, 1 mM EDTA, 1 mM dithiothreitol (DTT), 20 mM KCl, and 50 $\mu\text{g mL}^{-1}$ of BSA) and was incubated for 30 min at 30 °C. The loading buffer and the electrophoretic run were as described in Sambrook and Russel.²⁷ Water was used as negative control and 10 $\mu\text{g mL}^{-1}$ of poly-L-lysine (Sigma), which has the ability to bind to DNA, served as a positive control. Gel images were captured using an ImageQuant LAS 500 (GE Healthcare).

Combinatorial effect of FLC plus *CaThi* on *F. solani* growth

The assay was performed as described in the section “**Effect of *CaThi* on fungal growth**” with the indicated differences: 1×10^4 fungal conidia mL^{-1} were incubated on Sabouraud broth at 25 $\mu\text{g mL}^{-1}$ of FLC or at 5 $\mu\text{g mL}^{-1}$ of *CaThi*. Neither concentration inhibited the growth of the tested fungus. The combination of FLC (25 $\mu\text{g mL}^{-1}$) plus *CaThi* (5 $\mu\text{g mL}^{-1}$) was also tested. Control cells were grown in the absence of FLC and *CaThi* and also in the presence of individual concentrations. After the incubation period, all samples were analysed using DIC optical microscopy (Axioplan.A2, Zeiss). The assay was performed in triplicate. Fungal growth inhibition was evaluated by One-way ANOVA, and differences of the mean $p < 0.05$ were considered significant. All statistical analyses were performed using GraphPad Prism software (version 5.0 for Windows). Synergism is defined as a combined action of two or more substances that causes greater inhibition of the microorganism than the sum of the growth inhibition of the individual substances.

The fungicidal test was performed at the end of this assay. The total volume of control cells (without FLC and *CaThi*) was spread over the surface of the Sabouraud agar medium (in a Petri dish) with a Drigalski spatula and grown at 25 °C for 60 h. The

same procedure was followed with fungus treated with FLC ($25 \mu\text{g ml}^{-1}$) + *CaThi* ($5 \mu\text{g ml}^{-1}$) to verify cell viability. The Petri dishes were photographed after 60 h. The experiments were performed in triplicate, and the results are shown assuming that the control represents 100% viability.

RESULTS

Antifungal activity of *CaThi* against *F. solani* cells

As a first approach to analyse antifungal activity, we verified whether *CaThi* was able to inhibit *F. solani* conidial germination and mycelial growth. We observed that *CaThi* has strong antimicrobial activity against this fungus, and this activity was dose dependent. At concentrations of 50, 25 and $12.5 \mu\text{g mL}^{-1}$, *CaThi* was able to inhibit 83, 50 and 21%, respectively, of mycelial growth of the phytopathogenic fungus *F. solani* (Figure 1A). Based on these values, the IC_{50} of *CaThi* is $25 \mu\text{g mL}^{-1}$. Images of fungal cells were obtained after different growth times in the absence and presence of *CaThi* ($50 \mu\text{g mL}^{-1}$) (Figure 1B). The growth and development were observed for all control cells under these conditions, and the formation of hyphae from the germ tubes of the conidia was observed. For *F. solani* conidia treated with $50 \mu\text{g mL}^{-1}$ *CaThi*, the fungal growth pattern was completely different in time and in morphology from control samples. That is, for the same time interval, the *CaThi*-incubated conidia exhibited delayed hyphae germination and development, and several morphological alterations (smaller, slightly ramified with a rough aspect) in hyphae at the last time interval.

Based on this strong growth inhibition by *CaThi*, *F. solani* conidia viability was further analysed. We observed that treatment of *F. solani* conidia with $50 \mu\text{g mL}^{-1}$ of *CaThi* produced a severe reduction in the number of colony forming units detected after 48 h incubation. Hence, the peptide exerts a lethal effect, causing 72.8% death of *F.*

solani conidia (Figure 2). These results indicate that the inhibitory effect of *CaThi* on *F. solani* is based on its fungicidal action.

Plasma membrane permeabilization of *F. solani*

We observed in Figure 3 that after 12 h of incubation, *CaThi* ($50 \mu\text{g mL}^{-1}$) was able to permeabilize the plasma membrane of fungal conidia. This result was observed until 60 h of incubation; however, at as early as 24 h of incubation with *CaThi* we observed a gradual increase in propidium iodide labelling, which indicates that treated cells were dying. This is consistent with the previously determined fungicidal effect. A detailed inspection of Sytox green labelling images shows that nuclei presented a round globular morphology until 48 h but changed to spots of fluorescence at 60 h of *CaThi* treatment, suggesting DNA fragmentation.

***CaThi* induces oxidative stress**

Figure 4 shows that *CaThi* is able to induce the production of H_2O_2 . With only 10 min of incubation, we observed the formation of a brown precipitate inside cells where the DAB reaction with H_2O_2 occurred. After 20 min of treatment, increased colouring of this brown precipitate and its location were clearly observed, mostly at the tip of conidia. This labelling was observed until 1 h of incubation suggesting that up to that time *CaThi* still caused oxidative stress in the tested cells (Figure 4). The treatment of conidia with H_2O_2 as a positive control showed a very similar labelling pattern to that of *CaThi*.

Caspase activity is induced by *CaThi* in *F. solani*

To determine whether apoptosis occurs during the death of *F. solani* conidia induced by *CaThi*, the involvement of caspases was evaluated. FITC-VAD-FMK permeates the cell. In the cytoplasm, it functions as a pseudo-substrate that binds caspases at their active site, inhibiting them and becoming fluorescent in the process. Our results show that exposure of *F. solani* conidia to *CaThi* resulted in activation of caspases, indicated by green fluorescence, suggesting that apoptosis is involved (Figure 5). Propidium iodide (red fluorescence) labelling was most strongly detected after 24 h of *CaThi* incubation.

Localization of *Cathi* in *F. solani* cells

Next, we investigated whether *CaThi* is internalized in *F. solani* cells. For this, 20 $\mu\text{g mL}^{-1}$ of *CaThi*-FITC was used to verify an intracellular fluorescence signal, and the cells were also treated with DAPI to label nuclei. After 60 h of incubation, the intracellular fluorescence of *Cathi*-FITC was observed, indicating that the peptide penetrates fungal cells. However, *Cathi*-FITC did not produce a specific spot of fluorescence within the cell; overlapping *Cathi*-FITC images with DAPI did not indicate co-localization of these fluorescent signals (Figure 6).

***CaThi* binds DNA**

A previous study performed in the yeast *Candida tropicalis* suggested a possible target for *CaThi* in the cell nucleus.²² The previous report showed that *CaThi* is internalized in *F. solani*, raising the possibility that the peptide may interact with cellular DNA. This hypothesis was investigated by analysis of changes in DNA mobility. Our results indicate that, in the presence of 50, 25 and 12.5 $\mu\text{g mL}^{-1}$ of *CaThi*, the electrophoretic mobility DNA is altered compared to free DNA (Figure 7). This suggests that *CaThi*

can bind to DNA, retarding or preventing entry of the complex into the mesh of the agarose gel. This difference is visible by comparing the test (third lane) and positive control using poly L-lysine (second lane).

Effect of combined *CaThi* and FLC on the growth of *F. solani*

The effect of low doses of the peptide and the antimycotic FLC were tested separately and in combination. *CaThi* at $5 \mu\text{g mL}^{-1}$ only inhibited *F. solani* growth by 4%, and FLC at $25 \mu\text{g mL}^{-1}$ produced inhibition of 6% (Figure 8A). However, the same doses in combination (*CaThi* $5 \mu\text{g mL}^{-1}$ + FLC $25 \mu\text{g mL}^{-1}$) increased growth inhibition to 100%, indicating a synergistic activity between the two substances (Figure 8A). In Figure 8B, we show *F. solani* growth patterns in the presence of *CaThi* ($5 \mu\text{g mL}^{-1}$) or FLC ($25 \mu\text{g mL}^{-1}$) that are similar to control growth patterns (only fungi and medium), corroborating the results obtained by optical density readings (Figure 8A). However, the growth patterns of *F. solani* in the presence of a combination of *CaThi* and FLC (FLC ($25 \mu\text{g mL}^{-1}$) + *CaThi* ($5 \mu\text{g mL}^{-1}$)) showed a robust reduction in hyphae formation and elongation as observed under optical microscopy, resulting in no observable cell growth. We also observed an apparent change in hyphae morphology (Figure 8B). In the presence of both substances there was observable growth after 60 h of incubation. In contrast, in the control we observed a white mass of mycelia growing over the medium (Figure 8C). These data suggest that the effect of combining FLC and *Cathi*, at non-inhibitory concentrations for this fungus when used singly, completely blocks fungal growth.

DISCUSSION

Initially, in this work, we tried to determine the MIC of *CaThi* on the growth of the fungus *F. solani*. However, the MIC was not determined because of two main difficulties: first, the quantity of AMPs in plant tissues is relatively low, and second, AMPs are difficult to purify from extracts of plant tissues, turning the process laborious. These difficulties turn the yield of the purified peptide low.³⁶ This is the case of *CaThi* which is purified from *C. annuum* fruits. For this reason, at this moment we only have the option to use the natural peptide.

Therefore, here we analysed the antifungal activity of *CaThi* against the fungus *F. solani*. Our results showed that *CaThi* ($50 \mu\text{g mL}^{-1}$) causes a significant reduction in mycelial growth in addition to inhibition of conidia germination over 48 h of incubation (Figure 1). The concentration tested is the lethal dose, which kills 73% of *F. solani* conidia (Figure 2). Vila-Perelló *et al.*³⁷ showed that natural thionin from *Pyralia pubera* (Pp-TH) and its synthetic analogue have *in vitro* antimicrobial activity against various phytopathogenic bacteria and fungi at concentrations ranging from 0.3-3.0 μM (1.58-15.8 $\mu\text{g mL}^{-1}$). The viscotoxin *VtA₃* from *Viscum album* and other thionins were also able to inhibit germination of *F. solani* conidia at $50 \mu\text{g mL}^{-1}$, although this inhibition was analysed for 16 h of incubation. As for mycelial growth, $7.5 \mu\text{g mL}^{-1}$ of *VtA₃* was necessary to achieve 50% inhibition, and this potent activity was also verified against *Sclerotinia sclerotiorum* cells.³⁸ Studies have shown that the inhibitory concentration of AMPs varies widely and is dependent on the tested fungus. Van der Weerden *et al.*³⁹ showed that NaD1 defensin, another important AMP family isolated from *Nicotiana glauca*, inhibited 50% of mycelial growth of *F. oxysporum* and *Leptosphaeria maculans* and 65% of fungi *Thielaviopsis basicola*, *Verticillium dahliae* and *Aspergillus nidulans*, at a concentration of 1 μM ($5.3 \mu\text{g mL}^{-1}$). Our data, together with existing literature, reinforce the notion that thionins and other AMPs are active

plant compounds and promising candidates for the development of alternative treatments to combat plant disease.

The antifungal activity of thionins may be a direct result of protein-membrane interaction through the electrostatic interaction of positively charged thionins to negatively charged phospholipids in the fungal membranes. This interaction may result in the formation of pores or a specific interaction with a lipid domain, leading to membrane permeabilization. This membrane interaction make these molecules good models for understanding the mechanisms that lead to microorganism-induced cell death that causes disease in plants and animals.⁴⁰⁻⁴² Therefore, we analysed whether *CaThi* can impair the cytoplasmic membrane of *F. solani* conidia, leading to permeabilization. We observed that *CaThi* is able to permeabilize *F. solani* cells after 12 h of incubation (Figure 3). Thevissen *et al.*⁴⁰ demonstrated that when the hyphae of the fungi *Neurospora crassa* and *Fusarium culmorum* were grown in the presence of α -hordothionin, an antifungal thionin from barley seed, Ca^{2+} uptake increased, as did K^{+} efflux and medium alkalinity. Additionally, α -hordothionin caused permeabilization and altered the electrical properties of artificial lipid bilayers leading to their collapse. Giudici *et al.*⁴³ indicated that the viscotoxins *VtA₃* and *VtB*, members of the type III subclass of thionins, interact with model membranes containing negatively charged phospholipids and disrupt membranes in leakage assays. The same research group showed that approximately $50 \mu\text{g mL}^{-1}$ of *VtA₃* is able to modify the permeability of membranes of *F. solani* conidia using the probe Sytox green. These authors also observed that with only 5 min of incubation, fungal conidia were permeabilized and prolonged exposure of conidia to *VtA₃* progressively increased the percentage of permeabilized cells, reaching 70% in 30 min.³⁸ Taveira *et al.*²² demonstrated that *CaThi* was able to cause permeabilization in all six important *Candida* species tested,

suggesting that permeabilization may be the first in a sequence of cellular changes caused by *CaThi* that lead to the death of the microorganism. Our results are consistent with the observation that thionins inhibit fungal growth as a result of direct interactions with membranes. Nonetheless, more studies are crucial to determine the specific interaction of thionins with plasma membranes and understand their inhibitory properties.

Studies show that increased production of ROS in target organisms is a recurring mode of action employed by AMPs.⁴⁴⁻⁴⁶ In fungal cells, reactive oxygen species (ROS) such as superoxide radical ($O_2^{\cdot-}$), hydrogen peroxide (H_2O_2), and the hydroxyl radical (OH^{\cdot}) are reactive molecules generated as metabolic byproducts from endogenous or exogenous sources.^{47,48} These molecules, originating from oxygen intracellular metabolism, can act as signal transduction molecules, contributing to the activation of transcription factors.⁴⁹ Inside cells, ROS are normally in equilibrium with antioxidants; however, when this critical balance is disrupted, excessive generation of ROS results in significant cellular damage due to oxidative stress.⁵⁰ When analysing whether *CaThi* causes ROS (specifically H_2O_2) induction in *F. solani* conidia, we observed that within 10 min of incubation, H_2O_2 production increased and persisted until 60 min of incubation (Figure 4). Staining was most prominent in the tips of the conidia, where polar growth occurs. The ROS induction may be a consequence of the primary effect of membrane permeabilization, and together, these cell damages may be responsible for inhibition of germination of fungal conidia, viewed in the growth inhibition assay. Similar results were demonstrated to VtA3 thionin and *F. solani* interaction, including a suggestion that the production of ROS is due to the collapse of the cytoplasmic membrane in the presence of VtA₃.⁴⁴ Studying another family of plants AMPs, Aerts *et al.*⁴⁵ demonstrated that the defensin Rs-AFP2, induces the endogenous production of

ROS in cells of *C. albicans*. Those authors have demonstrated by the presence of the antioxidant ascorbic acid in the antimicrobial assay eliminates the Rs-AFP2 antifungal activity, suggesting a causal link between the antifungal activity of Rs-AFP2 and ROS production. Although six *Candida* species were analysed, *CaThi* was only able to induce ROS production in *C. tropicalis* cells.¹⁷ In this work, we demonstrated that *CaThi* induces the generation of ROS in fungal conidia, suggesting features in the mode of action common to other AMPs against various microorganisms.

Studies have shown that an endogenous ROS increase in early stages of the apoptotic process can lead to the destruction of various cell types through the apoptotic pathway.^{51, 52} Based on the increase of endogenous ROS in *F. solani* conidia induced by *CaThi*, we verified the detection of apoptosis in *F. solani* conidia treated with *CaThi* by assaying caspase activation, which is common in the early stages of apoptosis.⁵³ In this assay, we found that *CaThi* treatment was able to cause activation of caspases in *F. solani* conidia, indicating that programmed cell death may be triggered by *CaThi* in this fungus (Figure 5). Other AMPs isolated from different sources have been shown to induce apoptosis in yeast cell models.^{54, 55}

There is increasing evidence that plant AMPs, such as defensins, lipid transfer proteins (LTPs) and thionins, may enter and accumulate in the cytoplasm of yeast cells^{44,46,56} and may have intracellular targets.^{57, 58} Our results demonstrated *CaThi* is internalized in *F. solani* cells, possibly with an intracellular target that is still uncharacterized (Figure 6). *CaThi* binds to DNA *in vitro* (Figure 7) in all tested concentrations suggesting the target of *CaThi* may be DNA. Similar internalization results were shown for VtA₃ and *F. solani*⁴⁴ and NaD1 and *F. oxysporum* f. sp. vasinfectum³⁹ interactions. Additionally, Lobo *et al.*⁵⁸ treated the fungus *Neurospora crassa* with PsD1 (a plant defensin isolated from *Pisum sativum*) conjugated with FITC

to show its colocalization with DAPI *in vivo*. Therefore, this defensin targets the nucleus. It was also shown that PsD1 interacts with the cyclin F protein, which is associated with cell cycle control.³⁷ Taveira *et al.*²² demonstrated that CaThi is able to enter the cytoplasm of human pathogenic yeasts such as *C. albicans* and *C. tropicalis*, indicating a nuclear target for CaThi in cells of *C. tropicalis*. This work suggests that thionin toxicity is not restricted to the plasma membrane. Considering intracellular targets, studies show that once in the cytoplasm, AMPs can induce diverse cell damage, including inhibition of DNA, RNA, inhibition of protein synthesis, inhibition of cell wall synthesis and inhibition of enzyme activity.^{12, 57,59-61} The AMPs indolicitin and buforin II have also demonstrated the ability to bind directly to DNA.^{34, 62} It has been shown that wheat seed purothionin is able to block *in vitro* DNA synthesis through inhibition of the enzyme ribonucleotide reductase. It has been proposed that inhibition of DNA synthesis may explain the toxic effect of thionins against mammalian cells.⁶³ Additionally, the DNA binding capability of viscotoxins is related to the formation of complexes with negatively charged DNA, which protects DNA against thermal denaturation.⁶⁴ It has been suggested that the helix-turn-helix motif of viscotoxins may represent a DNA-binding domain.⁶⁵ However, it is still not possible to know whether these *in vitro* observations have significance *in vivo*, where the interaction is hampered by subcellular compartmentalization.

Fusarium fungi have high MICs to the available antifungal agents, including broad spectrum azoles. Even high doses of these antifungals do not interfere with normal development of this genus.^{26,28} In addition, high FLC doses are used worldwide to prevent and treat plant diseases caused by fungi. This use presents some drawbacks such as the generation of resistant fungal varieties, contaminate the soil and water affecting non target microorganisms,⁶⁶ and furthermore there is the hypothetical risk of

induced resistance in soil, plant and food dwelling microorganisms like *Coccidioides*, *Histoplasma*, *Aspergillus*, and *Cryptococcus* which are all human pathogens. If these resistant microorganisms infect humans, they may cause diseases more difficult to be treated.^{67, 68} Additionally, FLC was generally successful in treating *Candida* infections, despite reports of resistance that will preclude its future use.^{69,70} For these reasons, we selected FLC to test its efficacy combined with *CaThi*.

The results suggest that at combination of FLC and *CaThi*, both substances act in synergy (Figure 8A), prevent the development of conidia in hyphae (Figure 8B), and have fungicidal effects (Figure 8C). This evidence suggests that the combination of the two substances may severely disrupt cellular function. Morphological modification of conidia was observed under microscopic examination, indicating cell lysis. Taveira *et al.*²² showed the same synergistic effect of FLC with *CaThi* against six medically important *Candida* species; this combination caused drastic morphological changes in all cells.

The data suggest that the study of the combination of commercial drugs with plant AMPs is an interesting approach for developing new agricultural inputs for controlling fungal infections, since the combined use drastically reduces the concentration necessary to completely inhibit the *F. solani* growth and, therefore, this approach represents a possible treatment to these diseases that cause significant global crop losses without the drawbacks aforementioned. Additionally, *Fusarium* also causes severe localized and disseminated infections in immune-compromised patients^{28, 64}, making this study even more relevant as a new treatment possibility.

CONCLUSIONS

One of the most studied fungus genus is *Fusarium*, which contains some of the most important species of plant pathogens that economically affect agriculture and horticulture. A large number of *Fusarium* species cause infection in animals and humans in addition to plants. Therefore, the discovery of new antifungal agents is of paramount importance. Here, we demonstrated that *CaThi* has strong antifungal effect against *F. solani* by permeabilizing the membrane, inducing the oxidative stress response, activation of caspases and loss of viability in the fungus. We present evidence to suggest an intracellular target for *CaThi* that is still unknown. Our results show that combined treatment of *CaThi* and FLC is a strong candidate for studies to improve targeting of *F. solani*. This strategy is of particular interest because it minimizes selection of resistant microorganisms.

This study forms part of the DSc degree thesis of GBT, carried out at the Universidade Estadual do Norte Fluminense. We acknowledge the financial support of the Brazilian agencies CNPq, FAPERJ (E-26/102.362/2013; E-26/110.057/2014; E-26/202.132/2015, E-26/202.735/2016), CAPES through the CAPES/Toxinology project and CONICET from Argentina. The authors are grateful to L.C.D. Souza and V.M. Kokis for technical assistance.

REFERENCES

1. Strange, R. N.; Scott, P. R. *Annu Rev Phytopathol* 2005, 43, 83-116.
2. Makovitzki, A.; Viterbo, A.; Brotman, Y.; Chet, I.; Shai, Y. *Appl Environ Microbiol* 2007, 73, 6629-6636.

3. Kalpana, K.; Maruthasalam, S.; Rajesh, T.; Poovannan, K.; Kumar, K.K.; Kokiladevi, E.; Raja, J. A. J.; Sudhakar, D.; Velazhahan, R.; Samiyappan, R.; Balasubramanian, P. *Plant Sci* 2005, 170, 203-215.
4. Di Maro, A.; Terracciano, I.; Sticco, L.; Fiandra, L.; Ruocco, M.; Corrado, G.; Parente, A.; Rao, R. *J Biotechnol* 2010, 147, 1-6.
5. Xuan, T. D.; Yuichi, O.; Junko, C.; Eiji, T.; Hiroyuki, T.; Mitsuhiro, M.; Dang, K. T.; Hong, N. H. *Crop Prot* 2003, 22, 873-881.
6. Mahlo, S. M.; MCGaw, L. J.; Eloff, J. N. *Crop Prot* 2010, 29, 1529-1533.
7. Pane, C.; Piccolo, A.; Spaccini, R.; Celano, G.; Vilecco, D.; Zaccardelli, M. *Appl Soil Ecol* 2013, 65, 43-51.
8. Pelegrini, P. B.; Franco, O. L. *Int J Biochem Cell Biol* 2005, 37, 2239-2253.
9. Li, Y.; Xiang, Q.; Zhang, Q.; Huang, Y.; Su, Z. *Peptides* 2012, 37, 207-215.
10. Vriens, K.; Cammue, B. P. A.; Thevissen, K. *Molecules* 2014, 19, 12280-12303.
11. Kido, E. A.; Pandolfi, V.; Houllou-Kido, L. M.; Andrade, P. P.; Marcelino, F. C.; Nepomuceno, A. L.; Abdelnoor, R. V.; Burnquist, W. L.; Benko-Iseppon, A. M. *Curr Protein Pept Sci* 2010, 11, 220-230.
12. Castro, M. S.; Fontes, W. *Protein Pept Lett* 2005, 12(1), 13-18.
13. Balls, A. K.; Hale, W. S.; Harris, T. H. *Cereal Chem* 1942, 19, 279-281.
14. Stec, B. *Cell Mol Life Sci* 2006, 63, 1370-1385.

15. Bohlmann, H.; Clausen, S.; Behnke, S.; Giese, H.; Hiller, C.; Reimann-Philipp, U.; Schrader, G.; Barkholt, V.; Apel, K. *Embo J* 1988, 7, 1559-1565.
16. Lee, S.C.; Hong, J. K.; Kim, Y. J.; Hwang, B. K. *Physiol Mol Plant Pathol* 2000, 56, 207-216.
17. Berrocal-Lobo, M.; Molina, A.; Rodríguez-Palenzuela, P.; García-Olmedo F.; Rivas, L. *Exp Parasitol* 2009, 122(3), 247-249.
18. Broekaert, W.; F.; Cammue, B. P. A.; De Bolle, M. F. C.; Thevissen, K.; De Samblanx, G.; Osborn, R. W, *Crit Rev Plant Sci* 1997, 16(3), 297-323.
19. Tam, J. P.; Wang, S.; Wong, K. H.; Tan, W. L. *Pharmaceuticals* 2015, 8, 711-757.
20. García-Olmedo, F.; Molina, A.; Alamillo, J. M.; Rodríguez-Palenzuela, P. *Pept Sci* 1998, 47, 479-491.
21. Taveira, G. B.; Mathias, L. S.; Vieira-da-Motta, O.; Machado, O. L. T.; Rodrigues, R.; Carvalho, A. O.; Teixeira-Ferreira, A.; Perales, J.; Vasconcelos, I. M.; Gomes, V. M. *Biopolymers* 2014, 102, 30-39.
22. Taveira, G. B.; Carvalho, A. O.; Rodrigues, R.; Trindade, F. G.; Da Cunha, M.; Gomes, V. M. *BMC Microbiol* 2016, 16, 12.
23. Sanguinetti, M.; Posteraro, B.; Lass-Flörl, C. *Mycoses* 2015, 58, 2-13.
24. Price, C. L.; Parker, J. E.; Warrilow, A. G.; Kelly, D. E.; Kelly, S. L. *Pest Manag Sci* 2015, 71, 1054-1058.
25. Azevedo, M. M.; Faria-Ramos, I.; Cruz, L. C.; Pina-Vaz, C.; Rodrigues, A. G. *J Agric. Food Chem* 2015, 63, 7463-7468.

26. Nucci, M.; Marr, K. A.; Vehreschild, M.J.; de Souza, C. A.; Velasco, E.; Cappellano, P.; Carlesse, F.; Queiroz-Telles, F.; Sheppard, D. C.; Kindo, A.; Cesaro, S.; Hamerschlak, N.; Solza, C.; Heinz, W. J.; Schaller, M.; Atalla, A.; Arikan-Akdagli, S.; Bertz, H.; Galvão Castro, C, Jr.; Herbrecht, R.; Hoenigl, M.; Härter, G.; Hermansen, N. E.; Josting, A.; Pagano, L.; Salles, M. J.; Mossad, S. B.; Ogunc, D.; Pasqualotto, A. C.; Araujo, V.; Troke, P. F.; Lortholary, O.; Cornely, O. A.; Anaissie, E. *Clin Microbiol Infect* 2014, 20, 580-585.
27. Litvinov, N.; Silva, M. T. N.; van der Heijden, I. M.; Graça, M. G.; Oliveira, L. M.; Fu, L.; Giudice, M.; Aquino, M. Z.; Odone-Filho, V.; Marques, H. H.; Costa, S. F.; Levin, A. S. *Clin Microbiol Infect* 2015, 21, 268.e1-268.e7.
28. Stempel, J. M.; Hammond, S. P.; Sutton, D. A.; Weiser, L. M.; Marty, F. M. *OFID* 2015, 2, ofv099.
29. Broekaert, W. F.; Terras, F. R. G.; Cammue, B. P. A.; Vanderleyden, J. *FEMS Microbiol Lett* 1990, 69, 55-59.
30. Vieira, M. E. B.; Vasconcelos, I. M.; Machado, O. L. T.; Gomes, V. M.; Carvalho, A.O. *Acta Biochim Biophys Sin* 2015, 47, 716-729.
31. Thevissen, K.; Terras, F. R. G.; Broekaert, W. F. *Appl Environ Microbiol* 1999, 65(12), 5451-5458.
32. Thordal-Christensen, H.; Zhang, Z.; Wei, Y.; Collinge, D. B. *Plant J* 1997, 11, 1187-1194.
33. Liu, Z.; Zhang, Z.; Faris, J. D.; Oliver, R. P.; Syme, R.; McDonald, M. C.; McDonald, B. A.; Solomon, P. S.; Lu, S.; Shelver, W. L.; Xu, S.; Friesen, T. L. *PLoS Pathog* 2012, 8, e1002467.

34. Park, C. B.; Kim, H. S.; Kim, S. C. *Biochem Biophys Res Commun* 1998, 244, 253-257.
35. Sambrook, J.; Russell, D. W. *Molecular Cloning: A laboratory manual*; Cold Spring Harbor Laboratory Press, New York, 2001; 3rd ed.
36. Carvalho, A. O.; Gomes, V. M. *Curr Pharm Des* 2011, 17, 4270-4293.
37. Vila-Perelló, M.; Sánchez-Vallet, A.; García-Olmedo, F.; Molina, A.; Andreu, D. *FEBS Letters* 2003, 536, 215-219.
38. Giudici, A. M.; Regente, M. C.; Villalaín, J.; Pfüller, K.; Pfüller, U.; De La Canal L. *Physiol Plantarum* 2004, 121, 2-7.
39. van der Weerden, N. L.; Lay, F. T.; Anderson, M. *J Biol Chem* 2008, 283, 14445-14452.
40. Thevissen, K.; Ghazi, A.; De Samblanx, G. W.; Brownlee, C.; Osborn, R. W.; Broekaert, W. F. *J Biol Chem* 1996, 271(25), 15018-15025.
41. De Lucca, A. J.; Cleveland, T. E.; Wedge, D. E. *Can J Microbiol* 2005, 51, 1001-1014.
42. Nawrot, R.; Barylski, J.; Nowicki, G.; Broniarczyk, J.; Buchwald, W.; Goździcka-Józefiak, A. *Folia Microbiol* 2014, 59, 181-196.
43. Giudici, M.; Pascual, R.; de la Canal, L.; Pfuller, K.; Pfuller, U.; Villalaín, J. *Biophys J* 2003, 85, 971-981.
44. Giudici, M.; Poveda, J. A.; Molina, M. L.; De la Canal, L.; González-Ros, J. M.; Pfüller, K.; Pfüller, U.; Villalaín, J. *FEBS J* 2006, 273, 72-83.

45. Aerts, A. M.; François, I. E. J. A.; Meert, E. M. K.; Li, Q. T.; Cammue, B. P. A.; Thevissen, K. *J Mol Microbiol Biotechnol* 2007, 13, 243-247.
46. Mello, E. O.; Ribeiro, S. F. F.; Carvalho, A. O.; Santos, I. S.; Da Cunha, M.; Santa-Catarina, C.; Gomes, V. M. *Curr Microbiol.* 2011, 62, 1209-1217.
47. Waris, G.; Ahsan, H. *J Carcinog* 2006, 5, 1-8.
48. Kowaltowski, A. J.; de Souza-Pinto, N. C.; Castilho, R. F.; Vercesi, A. E. *Free Radic Biol Med* 2009, 47, 333-343.
49. Scandalios, J. G. *Trends Biochem Sci* 2002, 27, 483-486.
50. Scandalios, J. G. *Braz J Med Biol Res* 2005, 38, 995-1014.
51. Maiese, K.; Chong, Z. Z.; Hou, J.; Shang, Y. C. *Exp Gerontol* 2010, 45, 217-234.
52. De Felice, F. G.; Velasco, P. T.; Lambert, M. P.; Viola, K.; Fernandez, S. J.; Ferreira, S. T.; Klein, W. L. *J Biol Chem* 2007, 282, 11590-11601.
53. Zivna, L.; Krocova, Z.; Härtlova, A.; Kubelkova, K.; Zakova, J.; Rudolf, E.; Hrstka, R.; Macela, A.; Stulik, J. *Microb Pathog* 2010, 49, 226-36.
54. Hwang, B.; Hwang, J. S.; Lee, J.; Lee, D. G. *Biochem Biophys Res Commun* 2011, 405, 267-271.
55. Hwang, B.; Hwang, J. S.; Lee, J.; Kim, J. K.; Kim, S. R.; Kim, Y.; Lee, D. G. *Biochem Biophys Res Commun* 2011, 408, 89-93.

56. Zottich, U.; Da Cunha, M.; Carvalho, A. O.; Dias, G. B.; Silva, N. C. M.; Santos, I. S.; Nascimento, V. V.; Miguel, E. C.; Machado, O. L. T.; Gomes, V. M. *Biochim Biophys Acta* 2011, 1810, 375-383.
57. Brogden, K. A. *Nat Rev Microbiol* 2005, 3, 238-250.
58. Lobo, D. S.; Pereira, I. B.; Fragel-Madeira, L.; Medeiros, L. N.; Cabral, L. M.; Faria, J.; Bellio, M.; Campos, R. C.; Linden, R.; Kurtenbach, E. *Biochemistry* 2007, 46, 987-996.
59. Cudic, M.; Otvos, L. *Curr Drug Targets* 2002, 3, 101-106.
60. Li, S. S.; Gullbo, J.; Lindholm, P.; Larsson, R.; Thunberg, E.; Samuelsson, G.; Bohlin, L.; Claeson, P. *Biochem J* 2002, 366, 405-413.
61. Nicolas, P. *FEBS J* 2009, 276, 6483-6496.
62. Subbalakshmi, C.; Sitaram, N. *FEMS Microbiol Lett* 1998, 160, 91-96.
63. Nakanishi, T.; Yoshizumi, H.; Tahara, S.; Hakura, A.; Toyoshima, K. *Gan* 1979, 70, 323-326.
64. Woynarowski, J. M.; Konopa, J. *Physiol Chem* 1980, 361, 1535-1545.
65. Romagnoli, S.; Ugolini, R.; Fogolari, F.; Schaller, G.; Urech, K.; Giannattasio, M.; Ragona, L.; Molinari, H. *Biochem J* 2000, 350, 569-577.
66. Matthews, G. A. *Pesticide application methods*. Oxford: Blackwell Science, 2000; 3rd ed.
67. Hof, H. *Antimicrob Agents Chemother* 2001, 45, 2987-2990.

68. Azevedo, M. M.; Faria-Ramos Isabel.; Cruz, L.; Pina-Vaz, C.; Rodrigues, A. G. J Agric Food Chem 2015, 63(34), 7463-7468.
69. Cannon, R. D.; Lamping, E.; Holmes, A. R.; Niimi, K.; Baret, P. V.; Keniya, M. V.; Tanabe, K.; Niimi, M.; Goffeau, A.; Monk, B. C. Clin Microbiol Rev 2009, 22(2), 291-321.
70. Iwazaki, R. S.; Endo, E. H.; Ueda-Nakamura, T.; Nakamura, C. V.; Garcia, L. B.; Filho, B. P. A Van Leeuw 2010, 97, 201-5.

Legend:

FIGURE 1 (A) The effect of *CaThi* on the growth of the plant pathogen *Fusarium solani*. (-◇-) Control, (-□-) *CaThi* (50 $\mu\text{g mL}^{-1}$), (-△-) *CaThi* (25 $\mu\text{g mL}^{-1}$); (-×-) *CaThi* (12.5 $\mu\text{g mL}^{-1}$). (*) Indicates significance by the One-way ANOVA test ($P < 0.05$) which was calculated using by the absorbance values of experiment and its respective control. **(B)** Images of *F. solani* cells by light microscopy after different incubation times with *CaThi* (50 $\mu\text{g mL}^{-1}$). Control cells without *CaThi*. Bars = 20 μm , 63x objective. Experiments were performed in triplicate.

FIGURE 2 Lethal effect of *CaThi* on *F. solani* conidia. **(A)** Photographs of the Petri dishes showing the viability of conidia after the treatment with 50 $\mu\text{g mL}^{-1}$ of *CaThi* for 24 h. Bars = 1 cm. **(B)** The table shows the percentage of conidia death after the treatment with 50 $\mu\text{g mL}^{-1}$ for 24 h.

FIGURE 3 Membrane permeabilization assay. Images of *F. solani* cells after membrane permeabilization assay by fluorescence microscopy using the fluorescent probe Sytox green. Cells were treated with *CaThi* for 12, 24, 48 and 60 hours and then assayed for membrane permeabilization. All cells were also treated with the probe propidium iodide. Bars = 20 μm , 63x objective.

FIGURE 4 Hydrogen peroxide induction assay. Images of *F. solani* conidia after Hydrogen peroxide induction assay by light microscopy using the 3,3'-Diaminobenzidine (DAB) dye. Cells were treated with *CaThi* for 10 at 60 min and then assayed for Hydrogen peroxide induction. Positive control cells were treated only with Hydrogen peroxide (200 mM), negative control cells were incubated only water. Bars = 10 μm , 40x objective.

FIGURE 5 Detection of caspase activity induced by *CaThi*. Images showing the involvement of caspase activity in the fungal *F. solani* after 12 and 24 h incubation with 50 $\mu\text{g mL}^{-1}$ of *CaThi*. The control cells and cells treated with *CaThi* were incubated with CaspACE FITC-VAD-FMK and propidium iodide probes and analyzed by fluorescence microscopy. The green fluorescence indicates positive staining for caspase activity and red fluorescence indicating cell death. Bars = 20 μm , 63x objective.

FIGURE 6 Localization of *CaThi* in fungal cells. Images of *F. solani* cells incubated for 60 h with 20 $\mu\text{g mL}^{-1}$ *CaThi*-FITC by fluorescence microscopy. Nuclei were visualized by 4',6-diamidino-2-phenylindole dihydrochloride (DAPI) after the *CaThi*-FITC incubation period. Overlap of the DAPI and FITC images. Bars = 50 μm , 40x objective.

FIGURE 7 Electrophoretic visualization of DNA mobility in the presence of *CaThi* in 0.8% agarose gel. First lane, control (DNA and binding buffer) mobility of 100 ng of DNA; second lane (positive control), mobility of 100 ng DNA incubated 10 $\mu\text{g mL}^{-1}$ of poly-L-lysine; third lane, mobility of 100 ng DNA incubated with 50 $\mu\text{g mL}^{-1}$ *CaThi*, fourth line, mobility of 100 ng DNA incubated with 25 $\mu\text{g mL}^{-1}$ *CaThi*, fifth line, mobility of 100 ng DNA incubated with 12.5 $\mu\text{g mL}^{-1}$ *CaThi*. Negative image of the gel stained with GelRed.

FIGURE 8 Effect of subinhibitory concentrations of *CaThi*, FLC, and the combination of *CaThi* and FLC on *F. solani* growth and viability. **(A)** Growth inhibition assay. (-♦-) control (only medium and conidia); (-■-) *CaThi* (5 $\mu\text{g mL}^{-1}$); (-▲-) FLC (25 $\mu\text{g mL}^{-1}$); (-×-) FLC (25 $\mu\text{g mL}^{-1}$) + *CaThi* (5 $\mu\text{g mL}^{-1}$). Experiments were performed in triplicate. (*) Indicates significance by the One-way ANOVA test ($P < 0.05$) which was calculated by the absorbance values of the samples. **(B)** Images of *F. solani* cells by light

microscopy after the grown inhibition assay. The arrow indicates the point of cell lysis.

Bars = 20 μm , 40x or 63x objectives. (C) Cell viability assay. Control, images of the

Petri dishes showing the growth of *F. solani* (white mycelium) without FLC and *CaThi*.

FLC + *CaThi*, images of the Petri dishes showing the absence of growth of *F. solani*

after the treatment with FLC (25 $\mu\text{g mL}^{-1}$) in combination with *CaThi* (5 $\mu\text{g mL}^{-1}$) for

60 h (fungicide effect). Bars = 1 cm.

Accepted Article

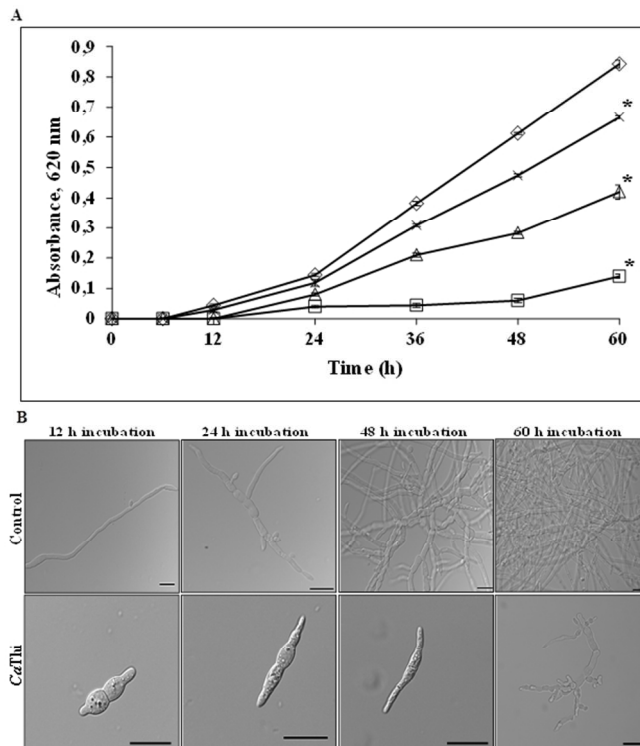


FIGURE 1 (A) The effect of CaThi on the growth of the plant pathogen *Fusarium solani*. (-◇-) Control, (-□-) CaThi (50 µg mL⁻¹), (-○-) CaThi (25 µg mL⁻¹); (-×-)CaThi (12.5 µg mL⁻¹). (*) Indicates significance by the One-way ANOVA test ($P < 0.05$) which was calculated by the absorbance values of experiment and its respective control. (B) Images of *F. solani* cells by light microscopy after different incubation times with CaThi (50 µg mL⁻¹). Control cells without CaThi. Bars = 20 µm, 63x objective. Experiments were performed in triplicate.

81x60mm (300 x 300 DPI)

Accel

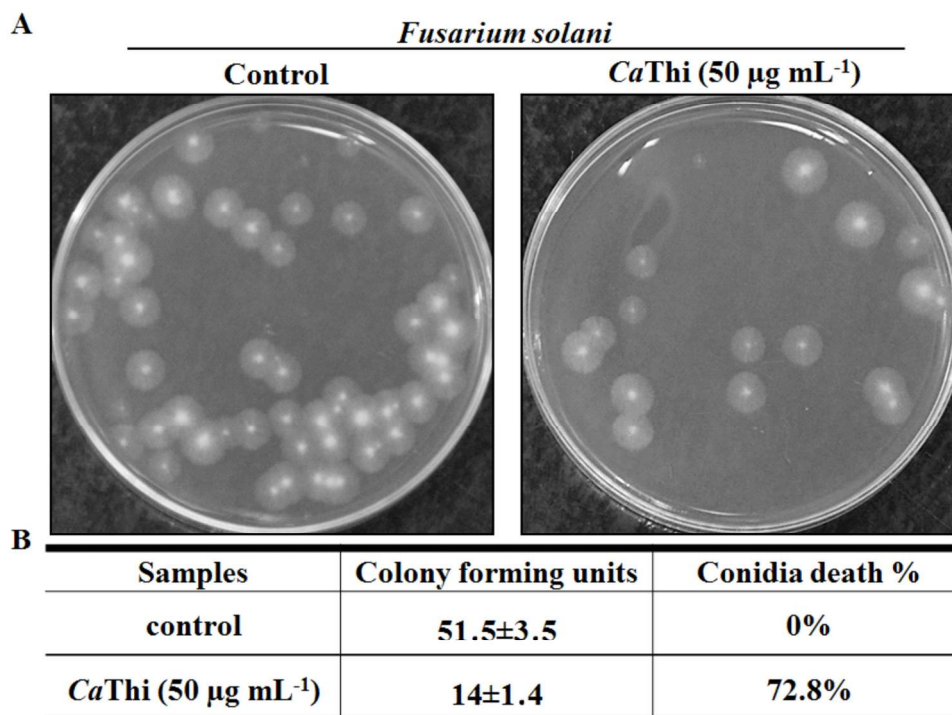


FIGURE 2 Lethal effect of CaThi on *F. solani* conidia. (A) Photographs of the Petri dishes showing the viability of conidia after the treatment with 50 µg mL⁻¹ of CaThi for 24 h. Bars = 1 cm. (B) The table shows the percentage of conidia death after the treatment with 50 µg mL⁻¹ for 24 h.

149x112mm (300 x 300 DPI)

Accep

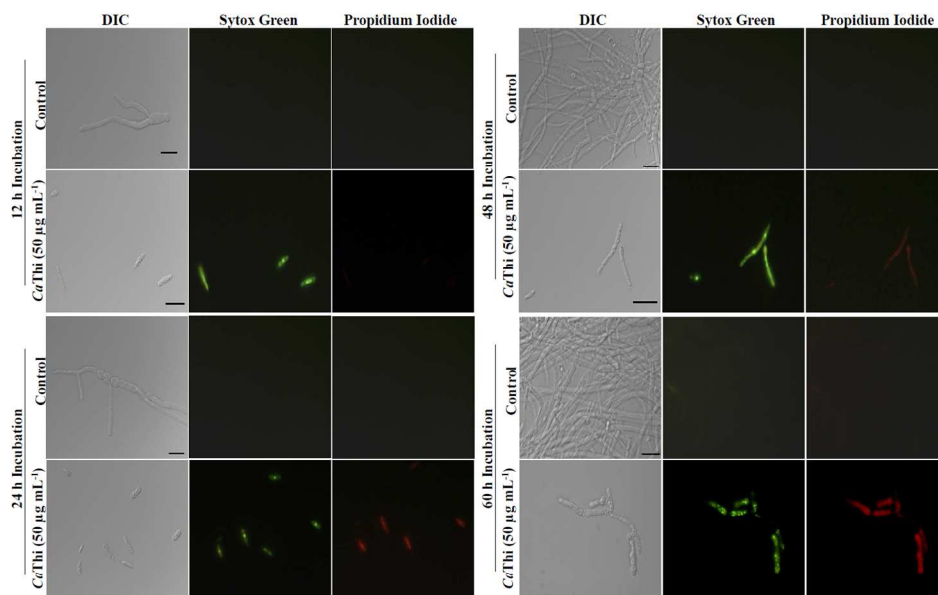


FIGURE 3 Membrane permeabilization assay. Images of *F. solani* cells after membrane permeabilization assay by fluorescence microscopy using the fluorescent probe Sytox green. Cells were treated with CaThi for 12, 24, 48 and 60 hours and then assayed for membrane permeabilization. All cells were also treated with the probe propidium iodide. Bars = 20 μm , 63x objective.

140x99mm (300 x 300 DPI)

Accep

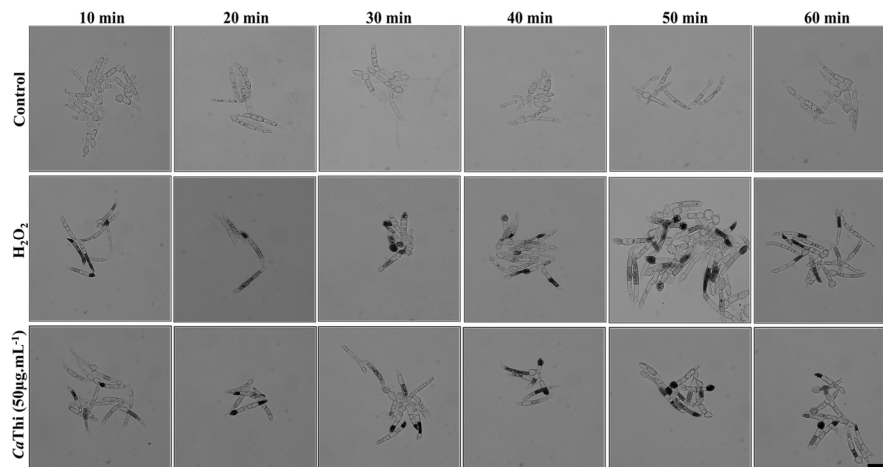


FIGURE 4 Hydrogen peroxide induction assay. Images of *F. solani* conidia after Hydrogen peroxide induction assay by light microscopy using the 3,3'-Diaminobenzidine (DAB) dye. Cells were treated with CaThi for 10 at 60 min and then assayed for Hydrogen peroxide induction. Positive control cells were treated only with Hydrogen peroxide (200 mM), negative control cells were incubated only water. Bars = 10 µm, 40x objective.

139x89mm (300 x 300 DPI)

Accept

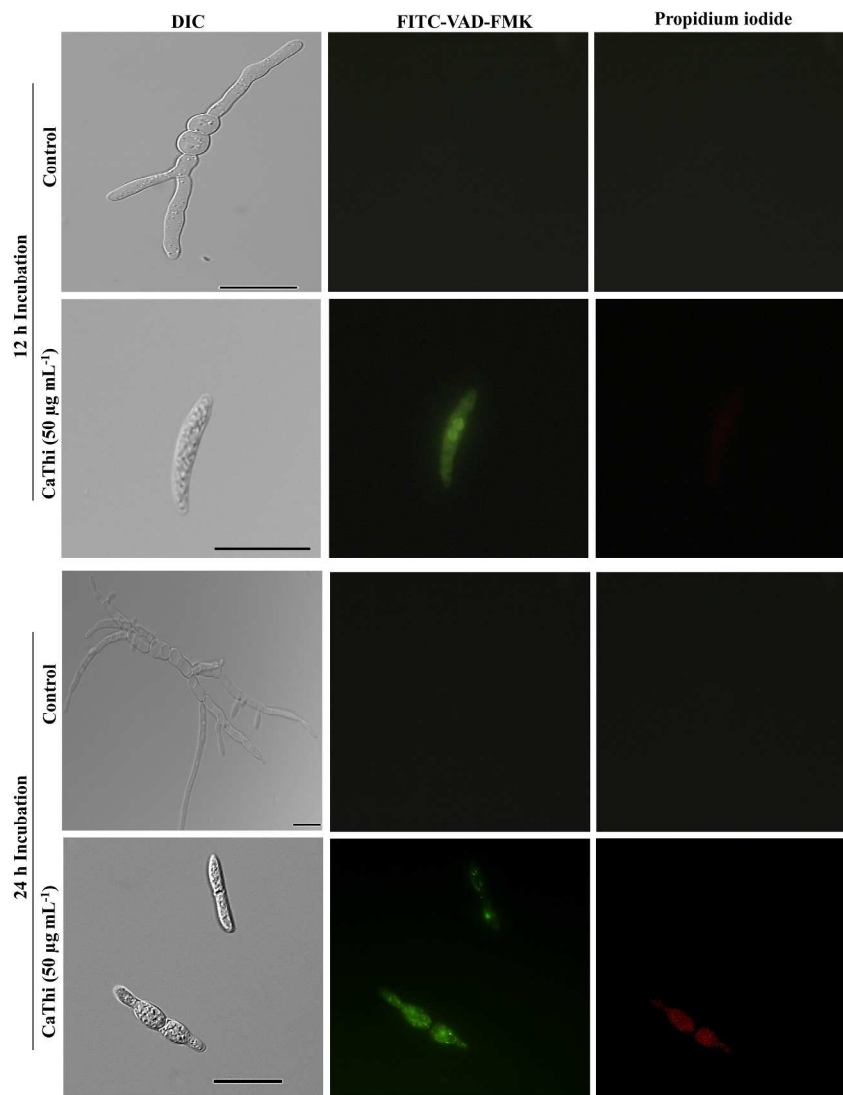


FIGURE 5 Detection of caspase activity induced by CaThi. Images showing the involvement of caspase activity in the fungal *F. solani* after 12 and 24 h incubation with 50 µg mL⁻¹ of CaThi. The control cells and cells treated with CaThi were incubated with CaspACE FITC-VAD-FMK and propidium iodide probes and analyzed by fluorescence microscopy. The green fluorescence indicates positive staining for caspase activity and red fluorescence indicating cell death. Bars = 20 µm, 63x objective.

250x312mm (300 x 300 DPI)

A

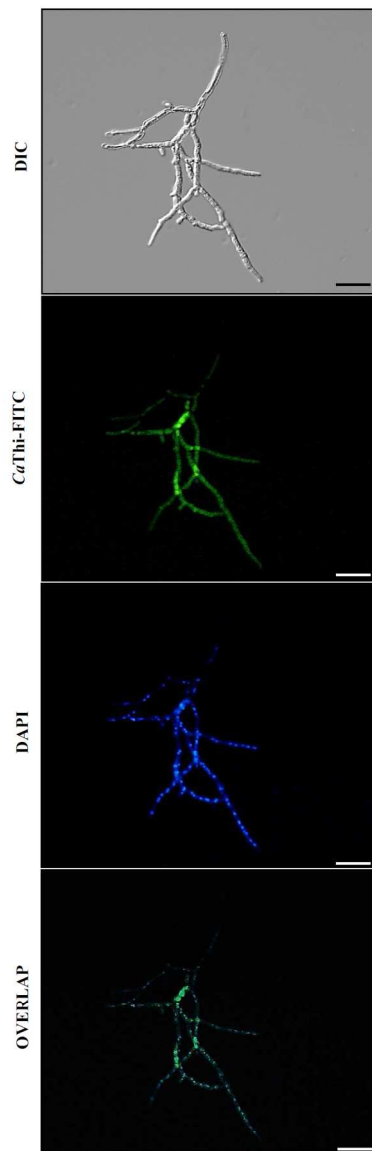


FIGURE 6 Localization of CaThi in fungal cells. Images of *F. solani* cells incubated for 60 h with $20 \mu\text{g mL}^{-1}$ CaThi-FITC by fluorescence microscopy. Nuclei were visualized by 4',6-diamidino-2-phenylindole dihydrochloride (DAPI) after the CaThi-FITC incubation period. Overlap of the DAPI and FITC images. Bars = $50 \mu\text{m}$, 40x objective.

90x189mm (300 x 300 DPI)

A

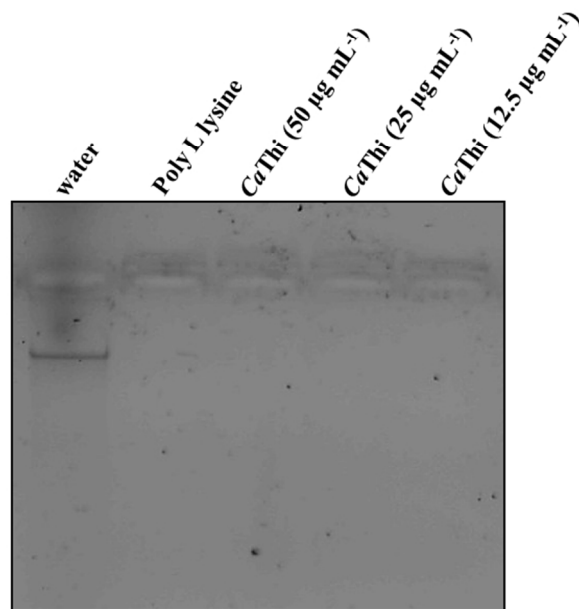


FIGURE 7 Electrophoretic visualization of DNA mobility in the presence of CaThi in 0.8% agarose gel. First lane, control (DNA and binding buffer) mobility of 100 ng of DNA; second lane (positive control), mobility of 100 ng DNA incubated 10 µg mL⁻¹ of poly-L-lysine; third lane, mobility of 100 ng DNA incubated with 50 µg mL⁻¹ CaThi, fourth line, mobility of 100 ng DNA incubated with 25 µg mL⁻¹ CaThi, fifth line, mobility of 100 ng DNA incubated with 12.5 µg mL⁻¹ CaThi. Negative image of the gel stained with GelRed.

81x60mm (300 x 300 DPI)

Accel

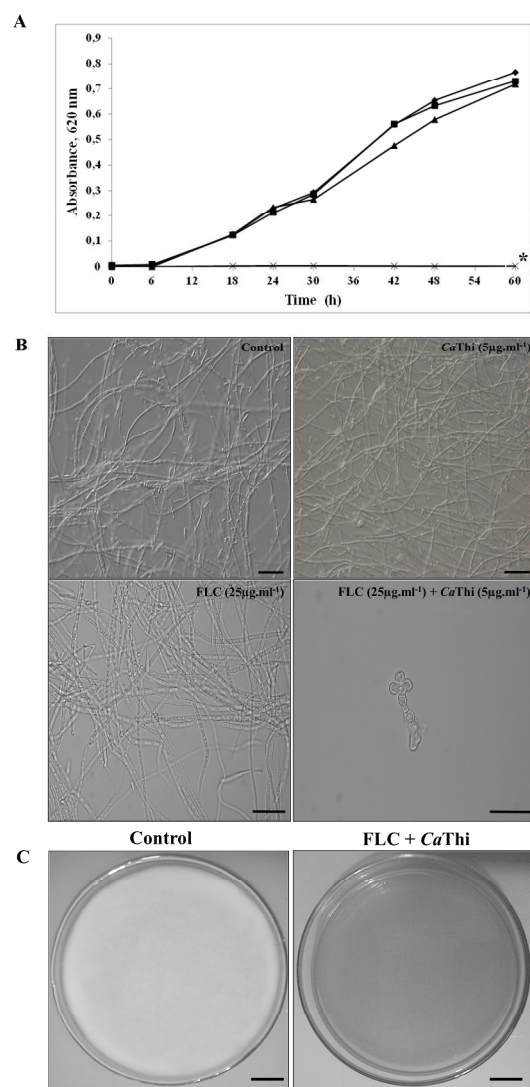


FIGURE 8 Effect of subinhibitory concentrations of CaThi, FLC, and the combination of CaThi and FLC on *F. solani* growth and viability. (A) Growth inhibition assay. (—♦—) control (only medium and conidia); (—■—) CaThi (5 µg mL⁻¹); (—▲—) FLC (25 µg mL⁻¹); (—×—) FLC (25 µg mL⁻¹) + CaThi (5 µg mL⁻¹). Experiments were performed in triplicate. (*) Indicates significance by the One-way ANOVA test ($P < 0.05$) which was calculated by the absorbance values of the samples. (B) Images of *F. solani* cells by light microscopy after the grown inhibition assay. The arrow indicates the point of cell lysis. Bars = 20 µm, 40x or 63x objectives. (C) Cell viability assay. Control, images of the Petri dishes showing the growth of *F. solani* (white mycelium) without FLC and CaThi. FLC + CaThi, images of the Petri dishes showing the absence of growth of *F. solani* after the treatment with FLC (25 µg mL⁻¹) in combination with CaThi (5 µg mL⁻¹) for 60 h (fungicide effect). Bars = 1 cm.

270x428mm (300 x 300 DPI)